ECCOMAS Congress 2016
VII European Congress on Computational Methods in Applied Sciences and Engineering
M. Papadrakakis, V. Papadopoulos, G. Stefanou, V. Plevris (eds.)
Crete Island, Greece, 5–10 June 2016

ON GRID RESOLUTION REQUIREMENTS FOR LES OF WALL-BOUNDED FLOWS

S. Rezaeiravesh[1], **M. Liefvendahl**[1,2] **and C. Fureby**[2]

[1] Division of Scientific Computing, Uppsala University, Sweden.
e-mail: saleh.rezaeiravesh@it.uu.se

[2] Swedish Defence Research Agency (FOI), Sweden.
e-mail: mattias.liefvendahl@foi.se, christer.fureby@foi.se

Keywords: Large-eddy simulation, Near-wall modelling, Grid point estimates, Turbulent boundary layers

Abstract. *Grid requirements for LES of wall-bounded flows are considered. The setting is a zero pressure gradient turbulent boundary layer on a flat plate, but the results are intended to be of use generally for the simulation of flows with an important influence of turbulent boundary layers. The basis for the grid estimates are expressions for the thickness and the viscous length scale of a turbulent boundary layer. The literature is reviewed, and a new power law is proposed, the coefficients of which have been determined using recent high-Re experimental data. An estimation for the number of grid points required for NWM-LES is derived, which is more general than previously published such estimates. A complete simulation methodology, including a numerical tripping device for transition to turbulence in the boundary layer, is demonstrated for NWM-LES of a flat plate turbulent boundary layer. The predictive accuracy is assessed by comparison with DNS data.*

1 INTRODUCTION

The number of application areas in which large-eddy simulation (LES) of turbulent flows is employed is currently growing rapidly, a development which is facilitated by the level of computational resources available today. The main alternative to LES for turbulent flows is Reynolds Averaged Navier-Stokes (RANS) modelling, which generally requires less computational resources since only the mean flow and turbulent quantities are computed. For free shear flows, there are compelling arguments for the use of LES. The main reason is that the energy cascade makes it possible to resolve a large part of the turbulent kinetic energy with a grid which is relatively coarse as compared to the viscous (Kolmogorov) length scale. Thus turbulent momentum transport, largely determined by the resolved scales, can be expected to be modelled more accurately by LES than RANS. Furthermore, since the large scale flow structures are directly simulated, LES provides significantly more information about the flow, as compared to RANS.

The present paper considers wall-bounded flows which put very different requirements on the simulation, as compared to free shear flows. The main reason for this is that the structure of turbulent boundary layers (TBLs) is quite different, as compared to turbulence away from walls. For instance, the peak in the Reynolds stress component $\langle u'u' \rangle$ occurs at $y^+ \approx 12$ in a zero pressure gradient (ZPG) TBL, e.g. [13]. Here u' are the fluctuations of the streamwise velocity, $\langle \cdot \rangle$ denotes averaging, and $y^+ = y/\delta_\nu$, where δ_ν is the viscous length scale. This fact has two implications, which are closely related, for the application of LES: *i)* energetic flow structures are present in the TBL on a length scale which is not very much larger than the viscous length scale, *ii)* with increasing Reynolds (Re-)number, the length scale of these flow structures decreases. Both of these items are in contrast to the free shear case, and make the application of LES to wall-bounded turbulence more difficult.

Three different broad approaches to LES of wall-bounded turbulence have generally been considered. *i)* Hybrid RANS-LES methods, where the TBL is modelled using RANS and the flow away from wall is modelled using LES. This means that the turbulence in the TBL is handled by the turbulence model, and that there are no resolved fluctuations in the TBL in the simulation. *ii)* Near-wall modelled (NWM-)LES in which the computational grid is constructed to resolve fluctuations the size of fractions of the TBL-thickness δ. The grid is, however, not adapted to the viscous length scale δ_ν, and the fluctuations in the innermost part of the TBL are handled by a near-wall model. This approach is in focus of the present paper. *iii)* Near-wall resolved (NWR-)LES in which the computational grid is constructed and adapted to resolve fluctuations the size of the viscous length scale.

For these three approaches it is clear that, from *i)* to *iii)*, more of the flow is directly resolved and less is handled by turbulence modelling. Associated with this is the rising computational cost caused by the increasing requirements on grid resolution. It is thus of utmost importance to precisely formulate the grid requirements and to have a good understanding of how they depend on the parameters of the flow problem, in particular the Re-number. It is the aim of the present paper to make a contribution to this, in particular for the case of NWM-LES.

Chapman derived grid requirements for RANS, NWM-LES and NWR-LES in a pioneering paper, [1]. However, as was pointed out by Choi and Moin [2] (see also section 3 of the present paper) the NWM-LES estimate is too optimistic, in that it leads to an underestimation of the required grid resolution. The reason for this is that in the derivation Chapman employed the mean (over the wall surface) thickness of the TBL. A more correct approach, as suggested by Spalart et al. [20], is to use the local TBL-thickness, and to obtain the grid estimate using

integration, as was done in [2], and also in section 3 of the present paper. A note on terminology: often these requirements are described as estimates on the number of grid points, or grid point estimates. The basis for the argument is however, both here and in [1, 2] is the grid length scale. Thus the derivations are equally applicable to grid points, grid elements (in the finite element framework), and grid cells (in the finite volume framework).

The paper is structured as follows. The basis for the grid estimates are expressions for the thickness δ and the viscous length scale δ_ν of the TBL. In section 2, the literature is reviewed, and new coefficient values are proposed for a power law form of the increase of the length scales with the downstream coordinate. The basis for the new coefficient values is a data fit to recent high-Re experimental data. Then, in section 3, a grid estimate is derived for NWM-LES, using the same approach as Choi and Moin [2]. The derivation is however more general in that it holds for any power law for δ, and the improved coefficients are then inserted in the final expressions. Furthermore, the form of the estimate is new, and it highlights the clustering of the grid in the initial length of the flat plate, for $\mathrm{Re}_x < 10^6$, approximately. In section 4, a complete simulation methodology is demonstrated for NWM-LES of a flat plate ZPG-TBL, with a length-based Re-number of $2.42 \cdot 10^6$, and a computational grid of $12 \cdot 10^6$ finite volume cells. This includes a numerical tripping device to induce resolved fluctuations in the boundary layer. The predictive accuracy of the simulation is assessed by comparison with data from DNS (direct numerical simulation). Throughout the paper, the setting is that of a ZPG-TBL on a flat plate. The grid estimates and the simulation methodology are however intended for application to a wide range of flow problems where TBLs have a significant role. This includes a large number of important applications in the marine, aeronautical and automotive engineering as well as other areas of research.

2 CORRELATIONS FOR TBL INTEGRAL QUANTITIES

For the purpose of grid estimation for NWM- and NWR-LES, it is required to express the boundary layer thickness δ and the viscous length scale $\delta_\nu = \delta/\mathrm{Re}_\tau = \nu/u_\tau$ in terms of the streamwise distance x measured from the leading edge of the plate or, equivalently, in terms of $\mathrm{Re}_x = U_0 x/\nu$, in which U_0 denotes the free-stream velocity. These quantities are interconnected through the definition of the friction coefficient,

$$c_f = 2\left(\frac{u_\tau}{U_0}\right)^2 = 2\left(\frac{\mathrm{Re}_\tau}{\mathrm{Re}_x}\right)^2 \left(\frac{x}{\delta}\right)^2. \tag{1}$$

A vast number of correlations to formulate the dependency of c_f on various Re-numbers have been proposed for the ZPG-TBL. They can be divided into several types according to their functional forms: *i)* power laws including the $1/5$th and $1/7$th ones [21] with the general form $c_f = c\mathrm{Re}^m$, *ii)* logarithmic laws $c_f = c_1(c_2 \log \mathrm{Re} + c_3)^m$ such as the suggestions of Schultz-Grunow [14], Schlichting [13], Frenholz-Finley [5], and White [21], and finally *iii)* other types such as the Prandtl-Kármán relation that can be found in [21, 13]. The coefficients and powers in each of these correlations were estimated using the experiential data available at the time, completely or partially combined with analytical methods. However, as more recent experimental data including those by Österlund [11] and Nagib et al. [9] came out, it was shown by Nagib et al. [10] that a major part of the existing correlations must be tuned up to achieve a good agreement with high Re-number experiments.

Among all the available correlations, we look for those having less deviation from available benchmark data, specifically at higher Re-numbers, while possessing a simple mathematical formulation making it possible to analytically evaluate integrals arising in the grid estimation

process, in section 3. The family of power law correlations is a suitable candidate satisfying the above demands. Dependency between each two quantities among δ/x, c_f, and different Re-numbers can be established given two starting correlations along with combination of (1) and the integral form of the streamwise momentum equation for ZPG-TBL which reads

$$c_f = 2\frac{d\theta}{dx} = 2\frac{d\mathrm{Re}_\theta}{d\mathrm{Re}_x}. \tag{2}$$

In Table 1, a summary of power law type correlations is presented. The oldest one is the $1/5$th law proposed by Prandtl in 1927 (as quoted in [21]), adjusted by low-Re experiments. The $1/7$th law is the outcome of combining White's [21] correlation, $c_f = 0.020\mathrm{Re}_\delta^{-1/6}$, derived from Coles' law of the wake [3] along with an assumption for θ/δ to be constant and equal to $7/72$, which corresponds to the $1/7$th velocity profile. In these relations, δ was supposed to be the theoretical thickness of the boundary layer. On the other hand, by combining the latter assumption with $c_f = 0.02358\mathrm{Re}_x^{-1/7}$ calibrated by Nagib et al. [10], the modified version of the $1/7$th law is derived.

In order to avoid making any presumption on the shape of velocity profile, it was chosen to tune up $c_f = c_1\mathrm{Re}_\delta^{-m_1}$ and $\delta/x = c_2\mathrm{Re}_x^{-m_2}$ based on Österlund's experimental observations [11] employing a least-squares technique and then derive other correlations using (1) and (2) without any further ad-hoc assumption. The boundary layer thickness was taken to be δ_{99} (δ at the point where TBL mean streamwise velocity becomes $0.99U_0$), which is a meaningful measurable quantity in an experiment or simulation. However, it was observed that employing the theoretical δ approximately obtained by plugging experimental values of c_f in Coles' law [3], for instance, would lead to very similar results for the derived correlations between $c_f - \mathrm{Re}_x$ and $c_f - \mathrm{Re}_\theta$.

Quantity	Suggestion	$1/5$th law, [21]	$1/7$th law, [21]	Modified $1/7$th law
c_f	$0.0283\mathrm{Re}_x^{-0.1540}$	• $0.058\mathrm{Re}_x^{-1/5}$	$0.027\mathrm{Re}_x^{-1/7}$	• $0.02358\mathrm{Re}_x^{-1/7}$, [10]
δ/x	• $0.1222\mathrm{Re}_x^{-0.1372}$	• $0.37\mathrm{Re}_x^{-1/5}$	• $0.16\mathrm{Re}_x^{-1/7}$	• $0.16\mathrm{Re}_x^{-1/7}$
c_f	• $0.01947\mathrm{Re}_\delta^{-0.1785}$	$0.0452\mathrm{Re}_\delta^{-1/4}$	• $0.02\mathrm{Re}_\delta^{-1/6}$	$0.0174\mathrm{Re}_\delta^{-1/6}$
Re_δ	$0.1222\mathrm{Re}_x^{0.8628}$	$0.37\mathrm{Re}_x^{4/5}$	$0.16\mathrm{Re}_x^{6/7}$	$0.16\mathrm{Re}_x^{6/7}$
Re_τ	$0.0145\mathrm{Re}_x^{0.7858}$	$0.063\mathrm{Re}_x^{7/10}$	$0.0186\mathrm{Re}_x^{11/14}$	$0.01737\mathrm{Re}_x^{11/14}$
Re_θ	$0.0167\mathrm{Re}_x^{0.8460} + c_\theta$	$0.0363\mathrm{Re}_x^{4/5}$	$0.01575\mathrm{Re}_x^{6/7}$	$0.01376\mathrm{Re}_x^{6/7}$

Table 1: Summary of the power law correlations for ZPG flat plate turbulent boundary layer. Symbol • represents the starting relations in each set. In the first column, $c_\theta = 373.83$.

The variation of c_f with Re_x and Re_θ estimated by different correlations is compared to the experimental measurements as well as direct numerical simulation (DNS) data from different sources over $5 \cdot 10^5 \leq \mathrm{Re}_x \leq 10^{10}$ in Figure 1. It immediately follows from the the proposed correlations that

$$c_f = 0.0134\left(\mathrm{Re}_\theta - c_\theta\right)^{-2/11},$$

which with a constant-value c_θ exhibits a good performance in the whole range of Re-numbers compared to DNS data [12, 16, 17] and experiments [11, 9].

It is noteworthy that at low Re-numbers only $c_f = 0.024\mathrm{Re}_\theta^{-1/4}$ given by Smits et al. [18] agrees with DNS of Schlatter and Örlü [12], besides the correlation suggested here. However, it, along with the $1/5$th law, diverges from the benchmark values and other curves as Re increases.

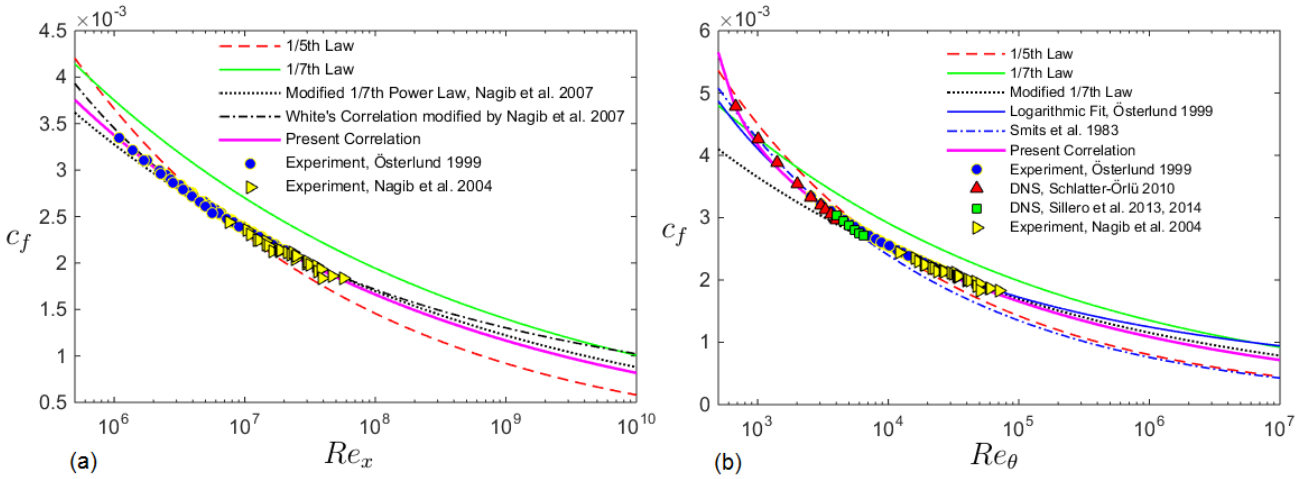

Figure 1: The friction coefficient, c_f, versus (a) Re_x and (b) Re_θ. White's correlation $c_f \approx 0.455\left[\ln(0.06\mathrm{Re}_x)\right]^{-2}$, [21], is modified by replacing 0.455 with 0.4177 as suggested by Nagib et al. [10]. Österlund's logarithmic fit: $c_f = 2\left[\frac{1}{\kappa} ln\mathrm{Re}_\theta + C\right]^{-2}$ with $\kappa = 0.384$ and $C = 4.08$ [11].

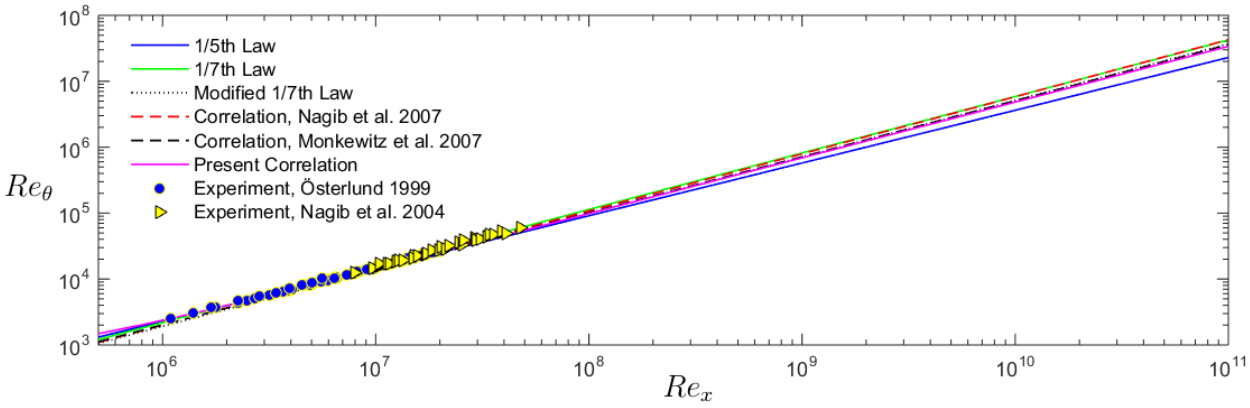

Figure 2: Re_θ versus Re_x predicted by correlations and given by experimtns.

Relatively better performance of the suggested $c_f - \mathrm{Re}_\theta$ curve at low Re-numbers is mainly due to the additive constant appearing when taking the integral of (2). By using the lowest Re-number data among Österlund's measurements [11], c_θ is predicted to be 373.83. This constant can also be seen as a single-point correction for x, taking into account the initial distance from the plate leading edge through which the boundary layer could have been laminar and then transited to turbulent. More detailed correction methods for the $\theta - x$ dependency can be found in [10, 8].

According to Figure 2, the deviation between various predictions increases with Re_θ which, along with lack of experimental evidence, makes it impossible to draw a conclusion on the best performance. However, as suggested by Nagib et al [10], for numerical estimation no preference can be given to any correlation at high Re-numbers, although it is observed that the modified $1/7$th and the suggested correlations are respectively the closest curves to $\mathrm{Re}_\theta = 0.016\mathrm{Re}_x^{0.85}$ fitted in $10^6 \leq \mathrm{Re}_x \leq 10^9$ by Monkewitz et al [8] to their detailed asymptotic expansion for $\theta(x)$, taking into account corrections for the virtual origin.

On the other hand, at high Re-numbers (say $\mathrm{Re}_x > 10^9$), the correlation $\mathrm{Re}_\theta = 0.01277\mathrm{Re}_x^{0.8659}$ proposed by Nagib et al. [10] behaves very closely to the 1/7th power law. But it must be em-

phasized again that a concrete comment regarding accuracy of different correlations at very high Re-numbers cannot be made.

3 A GRID ESTIMATE FOR NWM-LES

A grid estimate is derived in this section for NWM-LES of turbulent boundary layers. The setting is a flat-plate ZPG-TBL, but the estimate is intended to be useful for NWM-LES of flows with TBLs at curved walls as well. The derivation is applicable to any general unstructured grid generation approach which allows for a change of grid resolution throughout the computational domain. Isotropic grid elements/cells are considered, i.e. there is no systematic directional stretching of grid cells.

As was also the case in [1, 2], the starting point is an expression for the growth of the thickness of the TBL, along the flat plate, of the following power law form.

$$\delta(x) \approx \alpha x \mathrm{Re}_x^{\beta} = \alpha \left(\frac{U_0}{\nu}\right)^{\beta} x^{1+\beta} \tag{3}$$

In the previous section, different suggestions for the coefficients α and β were given and their agreement with experimental and DNS data was discussed. Note that another notation (c_i) was used there. The use of α and β here avoids subscripts. The derivation below is carried out without fixing the coefficient values and can hence be used with all such suggestions of the power law type.

A Cartesian coordinate system is used such that the free-stream velocity is directed in the positive x-direction, and the plate is located at, $0 < x < l$, $y = 0$, $0 < z < b$. Thus the length of the plate is l, and its width is b. The volume is divided into three different regions based on the characteristics of the flow. The first region, denoted V_1, is the fully developed TBL, $x_0 < x < l$, where equation (3) is an accurate description of the boundary layer thickness. Here x_0 is a suitably chosen location which has an important effect on the resulting grid estimate, as discussed below. The second region, denoted V_2, is the initial part of the boundary layer, $0 < x < x_0$. Typically, this includes laminar flow and then transition to turbulence in the boundary layer. Here, the situation is considered when the focus is on the TBL (and not on transition). Thus, it is only required to "initialize" the resolved fluctuations in the NWM-LES. How this can be done with a numerical tripping device is briefly illustrated in the next section. Finally, the third region is what remains of the domain in which the flow is to be simulated. This region is discarded from the grid estimate, as it is well-known that the grid resolution requirements are driven by the TBL, [1]. In the context of unstructured grid generation, a very significant coarsening of the grid can then be used outside of the boundary layer.

In order to obtain the grid estimate, the local cell density is introduced, $\rho_N(x) = \Delta N/\Delta V$. Here, ΔN is the number of cells in the volume ΔV. The total number of cells in a volume V is then obtained by integration,

$$N = \int_V \rho_N \, \mathrm{d}V. \tag{4}$$

For an unstructured grid with isotropic cells, and the cell size adapted to the local boundary layer thickness, the cell density is given by $\rho_N = n_0/\delta^3(x)$. Here n_0 is the target value for the number of cells in a cube with a side length equal to δ. In the literature, $10^3 < n_0 < 10^4$, is considered to be a suitable range for NWM-LES, [1, 20, 4]. For definiteness, $n_0 = 2\,500$, as suggested in the paper by Chapman, [1], is used below.

The required number of cells in region V_1 (the TBL) can now be estimated by,

$$N_1 = \int_0^b \int_0^{\delta(x)} \int_{x_0}^l \frac{n_0}{\delta(x)^3} \mathrm{d}x\mathrm{d}y\mathrm{d}z = bn_0 \int_{x_0}^l \frac{\mathrm{d}x}{\delta(x)^2} = \frac{bn_0}{\alpha^2} \left(\frac{\nu}{U_0}\right)^{2\beta} I_1, \tag{5}$$

where the integral I_1 is given by,

$$I_1 = \int_{x_0}^l \frac{\mathrm{d}x}{x^{2+2\beta}} = \frac{1}{1+2\beta}\left(\frac{1}{x_0^{1+2\beta}} - \frac{1}{l^{1+2\beta}}\right) < \frac{1}{1+2\beta}\frac{1}{x_0^{1+2\beta}} =: \bar{I}_1.$$

Here the last relation is used to define $\bar{I}_1$. The following somewhat surprising property is emphasized. In the limit $l \to \infty$, the integral I_1 is finite (and has the value $\bar{I}_1$), whereas it diverges as $x_0 \to 0$. Inserting the integral into equation (5) the grid estimate and its upper limit (denoted $\bar{N}_1$), are obtained in the following forms.

$$N_1 = \frac{n_0}{(1+2\beta)\alpha^2}\frac{b}{x_0}\left(\frac{1}{\mathrm{Re}_{x_0}^{2\beta}} - \frac{x_0}{l}\frac{1}{\mathrm{Re}_l^{2\beta}}\right) < \frac{n_0}{(1+2\beta)\alpha^2}\frac{b}{x_0}\mathrm{Re}_{x_0}^{-2\beta} =: \bar{N}_1 \tag{6}$$

It is clear from this estimate that there is a significant clustering of cells for $x \sim x_0$, whereas the grid cell coarsening for increasing x is rapid.

Next, the number of cells in the initial part of the boundary layer, region V_2, is estimated by assuming a constant cell density, $\rho_N = n_0/\delta^3(x_0)$, in a layer of constant thickness $\delta(x_0)$, which leads to,

$$N_2 = \frac{bx_0 n_0}{\delta^2(x_0)} = \frac{n_0}{\alpha^2}\frac{b}{x_0}\mathrm{Re}_{x_0}^{-2\beta}. \tag{7}$$

It is observed that the number of cells in this region is comparable to the number of cells in the TBL, i.e. $N_2/\bar{N}_1 = 1 + 2\beta$.

It is clear from the estimates (6) and (7) that x_0 is a crucial parameter. It was introduced above as a location after which the expression (3) is an accurate representation of the boundary layer thickness. This is however not an exactly defined location. For definiteness, $\mathrm{Re}_{x_0} = 5 \cdot 10^5$ is chosen, which is an approximate location of transition, and it is also a suitable choice for the type of "tripped" LES which is illustrated in the next section. Thus, Re_{x_0} is considered fixed and, $b/x_0 = \mathrm{Re}_b/\mathrm{Re}_{x_0}$, is inserted into the estimate for $\bar{N}_1$, see equation (6), to obtain,

$$\bar{N}_1 = \frac{n_0}{(1+2\beta)\alpha^2}\mathrm{Re}_{x_0}^{-1-2\beta}\mathrm{Re}_b.$$

From this expression, it is seen that it is the Re-number based on the plate width which determines the increase in grid cells with increasing Re-number. This fact was not clearly pointed out in previous investigations, [1, 20, 2]. Another interesting fact is that $\bar{N}_1$ grows linearly with Re_b, and that the coefficient β only affects the proportionality constant.

The growth in the number of grid cells with increasing Re-number is illustrated in Figure 3. Because of the role of x_0 in the estimates, graphs are shown for two different aspect ratios (b/l) of the plate, 4 and 1/4, respectively. Also included is the estimate from the paper by Chapman [1],

$$N_{Chap} = 40\frac{b}{l}n_0\mathrm{Re}_l^{0.4}, \tag{8}$$

and the estimate derived by Choi and Moin, [2],

$$N_{CM} = 54.7\frac{b}{l}n_0\mathrm{Re}_l^{2/7}\left[\left(\frac{\mathrm{Re}_l}{\mathrm{Re}_{x_0}}\right)^{5/7} - 1\right]. \tag{9}$$

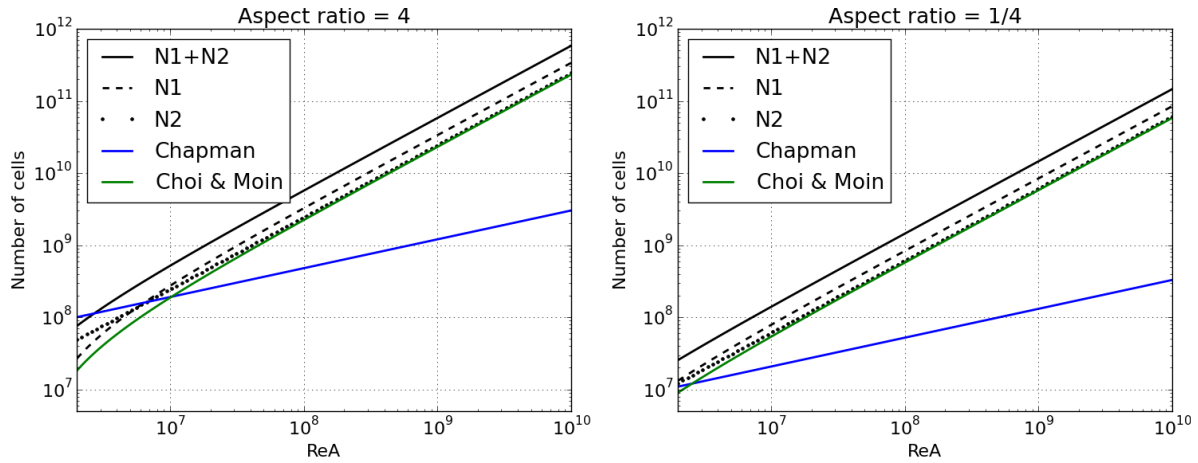

Figure 3: Grid estimates for a flat plate as a function of Re-number based on the plate area, $\mathrm{Re}_A = U_0\sqrt{bl}/\nu$. To the left the aspect ratio is $b/l = 4$, and to the right the aspect ratio is $b/l = 0.25$. The black lines (full, dashed, and dotted, respectively) show the estimates proposed in the present paper, where N_1 is given by equation (6), and N_2 is given by equation (7), and the parameters have the values $\alpha = 0.1222$, and $\beta = -0.1372$, see Table 1. The estimate by Chapman [1], blue line, is given by equation (8), and the estimate by Choi and Moin [2], green line, is given by equation (9).

As clearly illustrated in Figure 3, the estimate by Chapman is by far the most optimistic, in the sense that for high Re-numbers it leads to significantly lower estimates of the required number of grid cells. The main reason for this is that Chapman, [1], does not use integration, i.e. equation (4), to obtain the estimate. Instead an average boundary layer thickness over the whole plate is used. That it is more appropriate to use integration was pointed out in [20, 2], and the authors of the present paper agree with that assessment. Another remark is that the estimate by Choi and Moin [2], equation (9), only takes into account the part of the TBL downstream of x_0, whereas the estimate $N_1 + N_2$, also addresses the initial part of the boundary layer.

4 NWM-LES OF A FLAT PLATE TURBULENT BOUNDARY LAYER

This section contains a brief description of the computational set-up and results for one large-eddy simulation of a flat plate turbulent boundary layer. The first purpose is to illustrate what predictive accuracy can be expected with the mesh resolution levels discussed in the previous section. The second purpose is to demonstrate the practicality of the overall approach, including components such as the numerical tripping device used to induce resolved fluctuations in the boundary layer.

Quantity	Notation	Value	Unit
Length	l	2.000	m
Width	b	0.200	m
Height	h	0.133	m
Kin.visc.	ν	$1.65{\cdot}10^{-5}$	m^2/s
Velocity	U_0	20.4	m/s

Table 2: Parameters of the flat plate simulation. The plate has the aspect ratio 1/10, and the Reynolds numbers, Re_b=$2.42{\cdot}10^5$, and Re_l=$2.42{\cdot}10^6$.

The simulation case parameters are summarized in Table 4, and they lead to a length-based

Re-number of $\mathrm{Re}_l = 2.42 \cdot 10^6$. In fact, this corresponds to the TBL approaching the contoured ramp investigated by wind tunnel measurements in [19], and by LES in [7], which however is irrelevant for the present investigation. At the inflow boundary, a constant velocity U_0 is prescribed in the x-direction. A "strip" of grid cells is used for the numerical tripping device. In these cells the flow is perturbed by introducing a volume force in the momentum equation. The variation of the volume force is random in space and time. The TBL develops along the floor of the wind tunnel. On the lateral boundaries, periodic boundary conditions are used, and on the top boundary patch no-slip is used. The subgrid model employed is the One Equation Eddy Viscosity Model (OEEVM), [15, 7]. A wall model is used which modifies the viscosity in the cell-layer adjacent to the wall, as described in [6].

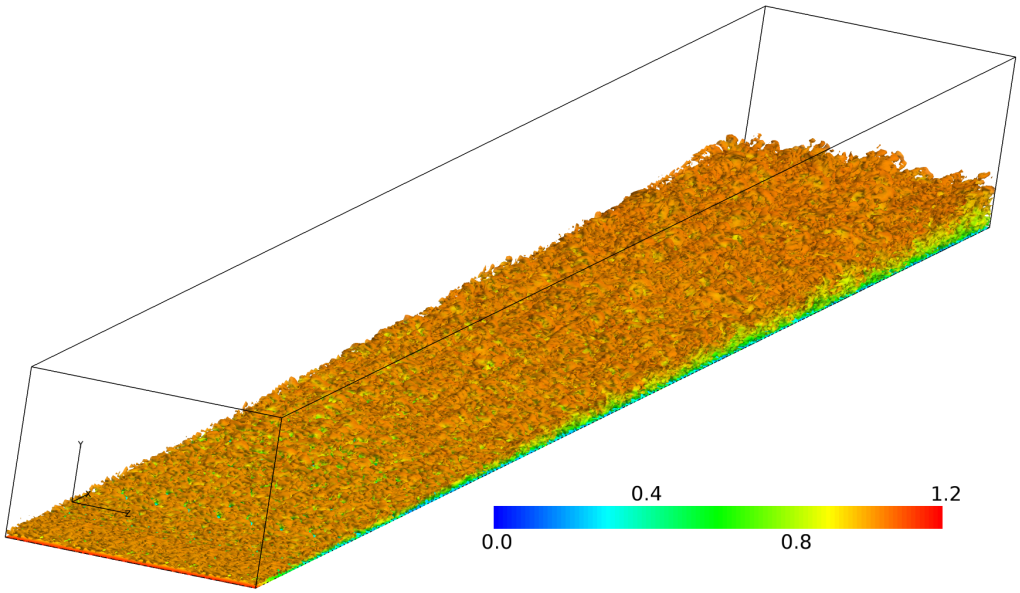

Figure 4: Illustration of the simulated TBL flow. An iso-surface of the second invariant of the velocity gradient is used to illustrate the turbulent structures in the boundary layer. The iso-surface is colored by the instantaneous normalized axial velocity, v_x/U_0. The black lines show the edges of the simulation domain.

A simple grid was used, which consists of hexahedral cells equal in size and shape throughout the domain. The number of cells was, $760 \times 160 \times 100$=12 160 000. This means that the grid adaption which is the basis of the grid estimates in the previous section, was not taken advantage of. However, the average grid resolution in the TBL in the simulation is similar to what is indicated in the grid estimates. Adopting the parameter values $\alpha = 0.1222$ and $\beta = -0.1372$, given in Table 1, N_1 and N_2 are estimated to be

$$\begin{aligned} N_1 &= 2.87 \cdot 10^6, \\ N_2 &= 3.03 \cdot 10^6, \end{aligned}$$

while employing Chapman's [1] and Choi-Moin's [2] approaches results in

$$\begin{aligned} N_{Chap} &= 3.61 \cdot 10^6, \\ N_{CM} &= 1.96 \cdot 10^6. \end{aligned}$$

Therefore, the simulation results give a rough indication of the level of accuracy which can be expected with the relevant grid resolution relative to the TBL thickness.

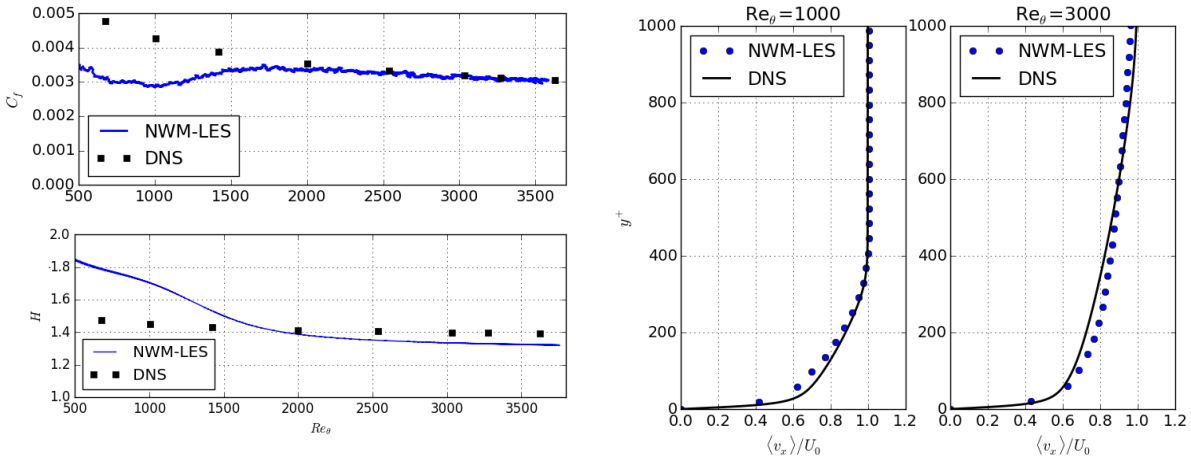

Figure 5: Left: Graphs for the friction coefficient c_f, and the shape factor H, as functions of Re_θ. Right: Profiles of the normalized mean velocity, $\langle v_x \rangle / U_0$, plotted versus y^+, at Re_θ = 1000 and 3000, respectively. Comparison of NWM-LES with DNS data, [12].

The flow is shown in Figure 4, by an iso-surface of an invariant of the instantaneous velocity gradient, to illustrate vortical structures in the TBL. In Figure 5, results from the NWM-LES are compared with DNS-data, [12]. The comparison includes the friction coefficient, the shape factor $H = \delta^*/\theta$ (i.e. the quotient of the displacement thickness and the momentum thickness), as well as mean velocity profiles at two stations along the flat plate. The curves for the friction coefficient and the shape factor clearly indicate the adaption length of the NWM-LES boundary layer. Overall, considering the significantly lower computational cost of the NWM-LES, as compared to DNS, the agreement of the results is quite good. A detailed elucidation of the discrepancies between the NWM-LES and DNS results is outside the scope of the present paper.

5 CONCLUDING REMARKS

A grid estimate has been derived for NWM-LES, as summarized in the expressions (6) and (7), for the number of grid cells in the initial length and the fully developed TBL, respectively. The derivation follows the approach of Choi and Moin [2], but it is more general as it holds for any power law for δ. Another novel feature is that an additional grid estimate is proposed for the initial length of the boundary layer, affected by transition. Furthermore, the grid estimate is formulated in a new way to highlight the clustering of the grid in the region starting from the leading edge of the plate up to $\mathrm{Re}_x \sim 10^6$.

New power law coefficients are also proposed, based on a data fit to recent high-Re experimental data. The coefficients are given in Table 1 together with a review of other proposed values from the literature.

In section 4, a complete simulation methodology is demonstrated for NWM-LES of a flat plate ZPG-TBL. The grid resolution level used in the simulation is comparable to that underlying the grid estimates. Note, however, that the type of grid coarsening and unstructured grid generation approach discussed in section 3 is not applied in the example simulation of section 4. The purpose of the simulation is to assess the predictive accuracy, with the relevant grid resolution relative to the boundary layer thickness. This is accomplished by comparing the friction coefficient, the shape factor and the mean velocity profile with DNS data.

ACKNOWLEDGEMENT

The authors wish to thank Timofey Mukha, at Uppsala University, for fruitful scientific discussions concerning the simulation of TBLs, and also for providing us with very convenient post-processing scripts. Niklas Wikström, at FOI, is thanked for the implementation of the simple and robust trip-model which was used in the simulation described in section 4. The work was supported by Grant No 621-2012-3721 from The Swedish Research Council.

REFERENCES

[1] D. R. Chapman. Computational aerodynamics development and outlook. *AIAA Journal*, 17:1293–1313, 1979.

[2] H. Choi and P. Moin. Grid-point requirements for large eddy simulation: Chapman's estimates revisited. *Physics of Fluids*, 24(1):011702, 2012.

[3] D. E. Coles. The law of the wake in the turbulent boundary layer. *J. Fluid Mech.*, 1:191–226, 1956.

[4] L. Davidson. Large Eddy Simulation: How to evaluate resolution. *International journal of Heat and Fluid Flow*, 30:1016–1025, 2009.

[5] H. H. Fernholz and P. J. Finley. The incompressible zero-pressure-gradient turbulent boundary layer: An assessment of the data. *Prog. Aerospace Sci.*, 32:245–311, 1996.

[6] C. Fureby, N. Alin, N. Menon, S. Svanstedt, and L. Persson. On Large Eddy Simulation of high Reynolds number wall bounded flows. *AIAA Journal*, page 457, 2004.

[7] C. Fureby, S. Zhu, and D. Jones. Large Eddy Simulation of the Flow over a Countoured Ramp. In *9th International Symposium on Turbulence and Shear Flow Phenomena*, Melbourne, Australia, 2015.

[8] A. Monkewitz, K. A. Chauhan, and H. M. Nagib. Self-consistent high-reynolds-number asymptotics for zero pressure- gradient turbulent boundary layers. *Phys. Fluids*, 19:115101, 2007.

[9] H. M. Nagib, C. Christophorou, and P. A. Monkewitz. High Reynolds number turbulent boundary layers subjected to various pressure-gradient conditions. In G. E. A. Meier and K. R. Sreenivasan, editors, *IUTAM Symp. on One Hundred Years of Boundary Layer Research*, pages 383–394. Springer, Berlin, 2004.

[10] H. N. Nagib, K. A. Chauhan, and P. A. Monkewitz. Approach to an asymptotic state for zero pressure gradient turbulent boundary layers. *Phil. Trans.R. Soc. A*, 365:755–770, 2007.

[11] J. M. Österlund. *Experimental studies of zero pressure-gradient turbulent boundary layer flow*. PhD thesis, Department of Mechanics, Royal Institute of Technology, Stockholm, 1999.

[12] P. Schlatter and R. Örlü. Assessment of direct numerical simulation data of turbulent boundary layers. *J. Fluid Mech.*, 659:116–126, 2010.

[13] H. Schlichting and K. Gersten. *Boundary Layer Theory*. Springer, Berlin, 8th edition, 2000.

[14] F. Schultz-Grunow. New frictional resistance law for smooth plates. *NASA Technical Memorandum*, 986, 1940.

[15] U. Schumann. Subgrid scale model for finite difference simulation of turbulent flows in plane channels and annuli. *J.Comp.Phys.*, 18(4):376–404, 1975.

[16] J. A. Sillero, Jiménez, and R. D. Moser. One-point statistics for turbulent wall-bounded flows at Reynolds numbers up to $\delta^+ \approx 2000$. *Phys. Fluids*, 25(105102), 2013.

[17] J. A. Sillero, Jiménez, and R. D. Moser. Two-point statistics for turbulent boundary layers and channels at Reynolds numbers up to $\delta^+ \approx 2000$. *Phys. Fluids*, 26(105109), 2014.

[18] A. J. Smits, N. Matheson, and P. N. Joubert. Low-Reynolds-number turbulent boundary layers in zero and favourable pressure gradients. *J. Ship Res.*, 27:147–157, 1983.

[19] S. Song, D. DeGraaff, and J. K. Eaton. Experimental study of a separating, reattaching and redeveloping flow over a smoothly contoured ramp. *Int. J. Heat and Fluid Flow*, 21(5):512–519, 2000.

[20] P. R. Spalart, W. H. Jou, M. Strelets, and S. R. Allmaras. Comments on the feasibility of LES for wings and on a hybrid RANS/LES approach. In *Advances in DNS/LES*, volume 1, pages 4–8, 1997.

[21] F. M. White. *Viscous Fluid Flow*. McGraw-Hill, New York, 3rd edition, 2005.